



# Multiple spatial scales of bacterial and fungal structural and functional traits affect carbon mineralization

Zhiyuan Ma<sup>1</sup>  | Shuo Jiao<sup>2</sup>  | Kaikai Zheng<sup>1,3</sup> | Haowei Ni<sup>1,3</sup> | Dong Li<sup>1,3</sup> | Na Zhang<sup>1,3</sup>  | Yunfeng Yang<sup>4</sup>  | Jizhong Zhou<sup>5,6</sup> | Bo Sun<sup>1</sup> | Yuting Liang<sup>1</sup> 

<sup>1</sup>State Key Laboratory of Soil and Sustainable Agriculture, Institute of Soil Science, Chinese Academy of Sciences, Nanjing, China

<sup>2</sup>State Key Laboratory of Crop Stress Biology in Arid Areas, College of Life Sciences, Northwest A&F University, Yangling, China

<sup>3</sup>University of the Chinese Academy of Sciences, Beijing, China

<sup>4</sup>State Key Joint Laboratory of Environment Simulation and Pollution Control, School of Environment, Tsinghua University, Beijing, China

<sup>5</sup>Department of Microbiology and Plant Biology, School of Civil Engineering and Environmental Sciences, Institute for Environmental Genomics, University of Oklahoma, Norman, Oklahoma, USA

<sup>6</sup>Earth and Environmental Sciences, Lawrence Berkeley National Laboratory, Berkeley, California, USA

## Correspondence

Yuting Liang, State Key Laboratory of Soil and Sustainable Agriculture, Institute of Soil Science, Chinese Academy of Sciences, Nanjing 210008, China.  
Email: [ytliang@issas.ac.cn](mailto:ytliang@issas.ac.cn)

## Funding information

National Natural Science Foundation of China, Grant/Award Number: 42107146 and 42377121; Natural Science Foundation of Jiangsu Province, Grant/Award Number: BK20210994; Innovation Program of Institute of Soil Science, Grant/Award Number: ISSASIP2201; Youth Innovation Promotion Association of the Chinese Academy of Sciences

**Handling Editor:** Kin-Ming (Clement) Tsui

## Abstract

Studying the functional heterogeneity of soil microorganisms at different spatial scales and linking it to soil carbon mineralization is crucial for predicting the response of soil carbon stability to environmental changes and human disturbance. Here, a total of 429 soil samples were collected from typical paddy fields in China, and the bacterial and fungal communities as well as functional genes related to carbon mineralization in the soil were analysed using MiSeq sequencing and GeoChip gene microarray technology. We postulate that CO<sub>2</sub> emissions resulting from bacterial and fungal carbon mineralization are contingent upon their respective carbon consumption strategies, which rely on the regulation of interactions between biodiversity and functional genes. Our results showed that the spatial turnover of the fungal community was 2–4 times that of the bacterial community from hundreds of meters to thousands of kilometres. The effect of spatial scale exerted a greater impact on the composition rather than the functional characteristics of the microbial community. Furthermore, based on the establishment of functional networks at different spatial scales, we observed that both bacteria and fungi within the top 10 taxa associated with carbon mineralization exhibited a prevalence of generalist species at the regional scale. This study emphasizes the significance of spatial scaling patterns in soil bacterial and fungal carbon degradation functions, deepening our understanding of how the relationship between microbial decomposers and soil heterogeneity impacts carbon mineralization and subsequent greenhouse gas emissions.

## KEYWORDS

carbon decomposition strategies, carbon mineralization, distance decay relationship, functional genes, greenhouse gas emission

## 1 | INTRODUCTION

Soil microorganisms are important engines of decomposition and participate in terrestrial carbon source-sink dynamics (Glassman et al., 2018; Jansson & Hofmockel, 2020; Nunan et al., 2020; Tang et al., 2018). Most soil microorganisms are heterotrophic and consume soil organic carbon (SOC) as energy, and this carbon mineralization process can accelerate the emission of CO<sub>2</sub> from soil to the atmosphere. Soil carbon mineralization is a critical process of the carbon cycle and is directly related to soil carbon quality (Chow et al., 2006; Lal, 2004). The special characteristics of the soil microbial community, including structural and functional traits, can lead to changes in carbon decomposition (Adair et al., 2008; Jackson et al., 2003). Bacteria and fungi are the two main groups of decomposing communities and show a variety of strategies affecting soil carbon sequestration and terrestrial carbon stability (Falkowski et al., 2008). For example, bacteria are the main decomposers of simple carbohydrates, organic acids, and amino acids (Myers et al., 2001), whereas fungi are more important than bacteria in decomposing refractory soil carbon (Fontaine et al., 2011). Refining the study of diverse carbon decomposition strategies employed by these microorganisms can yield a more comprehensive comprehension of how microbial-mediated soil-climate feedback operates. However, the potential far-reaching effects of heterogeneity on many aspects of microbial functional ecology have not been well understood or incorporated into our understanding of ecosystem functions in response to climate change at multiple spatial scales.

Spatial scales in ecology represent the biogeographic extent within which the mutual influences of neighbouring observations become effective. Species coexistence, which is fundamentally important for ecosystem function, is dependent on the spatial scale, and this relationship has been linked to the management of community diversity across landscapes (Hart et al., 2017). The scale dependence of ecological patterns is often induced by a sampling effect: increasing the scale of observation could increase the number of resources present and utilized so that species show a monotonic positive relationship with the scale of observation. Bruehlheide et al. (2018) found that the composition and driving force of the functional traits of communities differed between local areas (1–1000 m<sup>2</sup>) and large areas (25–12,500 km<sup>2</sup>), indicating that the ecological pattern depends on the spatial scale and exhibits a characteristic driving scenario. However, it remains unclear whether the spatial scales of different microbial taxa and their functional traits are important for maintaining ecosystem biogeochemical cycling. Carbon-degrading microbes in soil are fractal-like and tend to show self-similarity over some range of scales. The relative importance of elucidating differences in community similarity across spatial scales and quantifying the impact of different community compositions on carbon mineralization processes should be linked to ecological functions.

The distance decay relationship (DDR) is a common biogeographic model in ecology that refers to the decrease in community

similarity with geographic distance (Green et al., 2004; Horner-Devine et al., 2004). The DDR of microbial community composition has been investigated at regional (Green et al., 2004; Griffiths et al., 2011), continental (Lauber et al., 2008), and global (Tedersoo et al., 2012) scales. This relationship varies among different microbial taxonomic groups. By examining the DDR of soil diazotrophic and bacterial communities from 1 m–700 km, it was found that DDR slopes (spatial turnover rate) were steeper for diazotrophs than for bacteria (Gao et al., 2019). For the factors affecting the composition of microbial communities that cause different DDR patterns, it is generally believed that the important roles of selection and dispersion as well as drift and diversification have significant effects (Ning et al., 2020). Environmental filtering, driven by factors such as pH and the SOC and NH<sub>4</sub><sup>+</sup> contents, affects the spatial pattern of soil microorganisms (Jiao et al., 2019; Liu et al., 2015; Yao et al., 2013). Probabilistic dispersal can affect DDR patterns independently of niche differences (Wang et al., 2017). At present, research on soil microorganisms is moving forward from community composition to functional traits (Fierer & Jackson, 2006; Grundmann & Debouzie, 2000; Nunan et al., 2002; Ritz et al., 2004). However, it is still unclear how the spatial scale and functional characteristics of different microbial groups affect soil carbon stability.

Paddy soils cover 150 million ha globally (GRISP, 2013), representing one of the world's most important agricultural ecosystems. This wide distribution area can provide an ideal habitat for studying microbial functional traits at wide spatial scales. In this study, we collected a total of 429 soil samples from paddy fields throughout rice cropping regions in China. Soil bacterial and fungal communities and carbon-degrading functional genes were analysed by 16S rRNA and ITS amplicon sequencing and a high-throughput functional gene array GeoChip (Zhou et al., 2015). A spatial sampling design was used to realize the balanced distribution of paired distances at different spatial scales, i.e., local scale (1–100 m), mesoscale (0.5–50 km), regional scale (100–3500 km), and overall scale (1 m–3500 km). Here, we propose that the participation of diverse microorganisms in carbon mineralization is contingent upon the carbon consumption strategies exhibited by bacteria and fungi at varying spatial scales, with these strategies being influenced by the trade-off between biodiversity and functional genes. Our study suggested the importance of spatial scaling patterns of soil bacterial and fungal carbon degradation functions, which can deepen the understanding of how the relationship between microbial decomposers and soil heterogeneity affects carbon mineralization and subsequent greenhouse gas emissions.

## 2 | MATERIALS AND METHODS

### 2.1 | Sampling and site characteristics

Soil samples were collected across China from typical paddy fields. In total, 39 paddy fields in 13 regions (three plots per region) were selected to cover a wide spatial extent, from 110°10' and 126°14'E

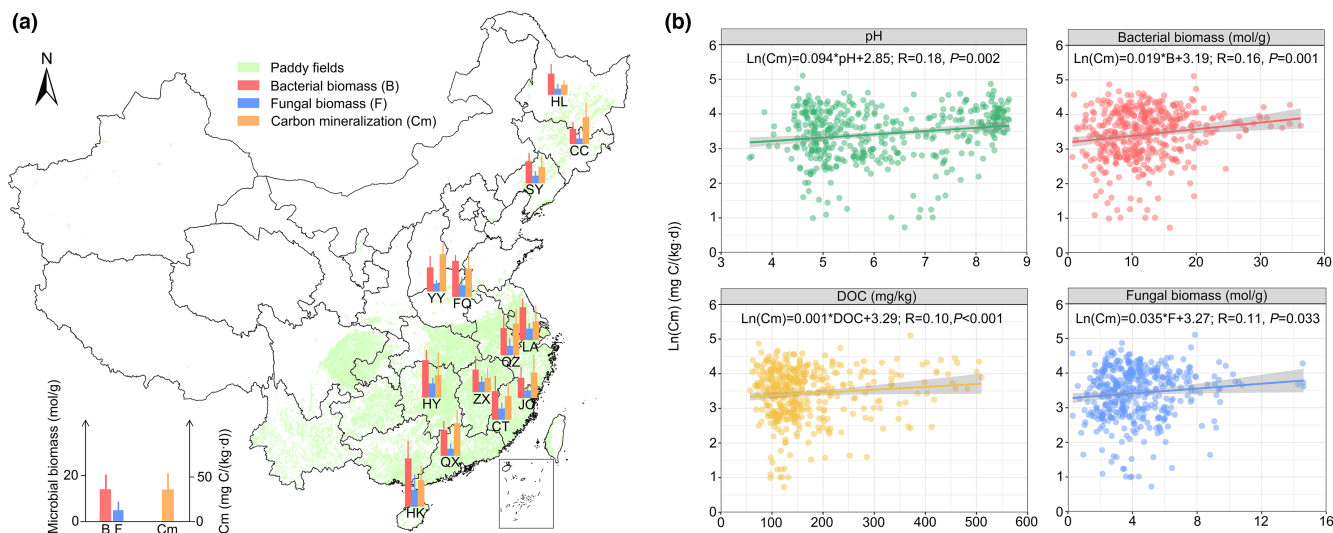


**FIGURE 1** Scenario of carbon mineralization and significant correlations between abiotic and biotic factors in typical paddy fields across China. (a) Carbon mineralization and bacterial and fungal biomasses at different latitudes. The column represents the mean values of bacterial biomass (mol/g), fungal biomass (mol/g), and carbon mineralization (mg/(kg d)) of 33 parallel soil samples (triplicates with 11 biological replicates) among 13 sampling sites, and the error bar represents the standard deviation; (b) relationships between carbon mineralization and pH, dissolved organic carbon (DOC), bacterial biomass, and fungal biomass based on Pearson correlation analyses. The shaded areas show the 95% confidence interval.

in longitude and  $19^{\circ}32'$  and  $46^{\circ}58'N$  in latitude (Figure 1). The mean annual temperature (MAT) in the region ranges from  $1.5^{\circ}C$  to  $23.8^{\circ}C$ , and the mean annual precipitation (MAP) ranges from 399 mm to 2216 mm. In brief, 11 soil samples (biological replicates) were collected with well-designed pairwise distances for each field. Six soil samples were collected along a 75 m long soil transect, and an additional five samples were collected along a vertical 75 m long transect. The distance between two adjacent samples along both transects was 1, 5, 10, 20, or 40 m. Each soil sample was combined with five soil cores taken at a depth ranging from 0 to 15 cm, and the litter layer was not included in the soil sampling. All soil samples were sealed in sterile sampling bags, transported to the laboratory on ice, and divided into two subsamples within 48 h. One subsample was kept at  $4^{\circ}C$  for measuring the soil properties (Table S1), and the other was stored at  $-80^{\circ}C$  for molecular analysis.

## 2.2 | Climatic and soil physicochemical properties, soil carbon mineralization, and microbial biomass analysis

The climate attributes, including MAT and MAP, were obtained from the meteorological observation database of the experimental stations. The soil pH was determined with a glass electrode at a 2.5:1 water: soil ratio. A 0.5-M  $K_2SO_4$  extract was prepared to determine the dissolved organic carbon (DOC) content and measured using a Multi N/C 2100 analyser (Analytik Jena, Germany). Total nitrogen, nitrate ( $NO_3^-$ -N), and ammonium nitrogen ( $NH_4^+$ -N) contents were measured by the Kjeldahl method (Bremner, 1965). Soil total

P (TP) was digested with  $HF-HClO_4$  and then determined using the molybdenum-blue method with an atomic absorption spectrophotometer (Zeenit 700P, Analytik Jena AG, Germany).

Soil  $CO_2$  respiration is regarded as carbon mineralization (Haney et al., 2008; Xiao et al., 2018). Soil  $CO_2$  respiration was measured using the static alkali absorption method (Yim et al., 2002). Twenty grams of fresh soil was weighed into a 250 mL plastic bottle, deionized water was added to adjust the level to 60% of the maximum field capacity, and an absorption bottle containing NaOH absorption solution was placed in a plastic bottle. The  $CO_2$  produced by soil respiration was collected. The bottle was sealed and placed in a constant-temperature incubator at  $28^{\circ}C$  and protected from light for continuous culture. The absorption solution was removed at intervals to determine the NaOH content, and the acid-base titration method was used to determine the NaOH content. Phenolphthalein was used as the indicator. The concentrations of NaOH in the absorption solutions of the control group (without soil and only the absorption solution in the plastic bottle) and the experimental group were the amount of  $CO_2$  respiration ( $R_H$ ) in the soil during this period. The  $R_H$  values ranged from 0.08 mg/(kg h) to 25.20 mg/(kg h).

Phospholipid fatty acid analysis (PLFA) was performed according to standard protocols (Bossio & Scow, 1998). The main steps were as follows. Fresh soil was extracted with an extract (chloroform:methanol:phosphate buffer volume ratio = 1:2:0.8) and then eluted with chloroform, acetone, and methanol. The phospholipids were separated and extracted, and then methanol was esterified to form fatty acid methyl ester. The contents of various fatty acids were determined by gas chromatography. The MIDI software system was used to analyse the soil microbial biomass and its community structure.

## 2.3 | Soil DNA extraction and MiSeq sequencing

Soil DNA was extracted from 2 g of well-mixed soil for each sample by combining freeze-grinding and sodium dodecyl sulphate for cell lysis as previously described (Zhou et al., 1996). The quality of the extracted DNA was assessed according to the 260/280 nm and 260/230 nm absorbance ratios by a Nanodrop 2000 (Thermo Fisher Scientific, Wilmington, DE, USA). All DNA was stored at  $-80^{\circ}\text{C}$ .

For bacteria, the primers 338F (ACTCCTACGGGAGGCAGCA) and 806R (GGACTACHVGGGTWTCTAAT) were used to amplify the V3-V4 region of the 16S rRNA gene (Lee et al., 2012). For fungi, the primers ITS1-1737F (GGAAGTAAAAGTCGTAACAAGG) and ITS2-2043R (GCTGCGTTCTTCATCGATGC) were used to amplify the ITS1 region of the ribosomal RNA gene (Degnan & Ochman, 2012). Both forward and reverse primers were tagged with adapter, pad, and linker sequences. A barcode unique to the reverse primer was added to permit the multiplexing of samples (GCCAAT for bacteria and CTTGTA for fungi) (Mazurkiewicz et al., 2006). An ABI GeneAmp® 9700 (ABI, Foster City, CA, USA) with a 20  $\mu\text{L}$  reaction system containing 4  $\mu\text{L}$  of 5 $\times$  FastPfu Buffer, 0.8  $\mu\text{L}$  of each primer (5  $\mu\text{M}$ ), 2  $\mu\text{L}$  of 2.5 mM dNTPs, 10 ng template DNA, and 0.4  $\mu\text{L}$  FastPfu Polymerase was used to perform the polymerase chain reaction (PCR) amplification. The PCR protocol for bacteria consisted of an initial predenaturation step at  $95^{\circ}\text{C}$  for 3 min, 28 cycles of 30 s at  $94^{\circ}\text{C}$ , 30 s at  $55^{\circ}\text{C}$ , and 45 s at  $72^{\circ}\text{C}$ , and a final 10 min extension at  $72^{\circ}\text{C}$ . The amplification steps for the ITS were similar to those of the 16S rRNA genes except for the changes in the PCR conditions, in which the initial predenaturation was at  $95^{\circ}\text{C}$  for 3 min, followed by 35 cycles of 30 s at  $95^{\circ}\text{C}$ , 30 s at  $59.3^{\circ}\text{C}$ , and 45 s at  $72^{\circ}\text{C}$ , and a final 10 min extension at  $72^{\circ}\text{C}$ . Three PCRs were conducted for each sample. They were combined after PCR amplification. The PCR products were separated on a 2.0% agarose gel. We excised and purified the band of the correct size using an AxyPrep DNA Gel Extraction Kit (Axygen Scientific, Union City, CA, USA), and quantification was performed with QuantiFluor™-ST (Promega, Madison, WI, USA).

The pooled DNA was diluted to 2 nM, loaded onto the reagent cartridge, and run on a MiSeq benchtop sequencer (Illumina Inc., San Diego, CA, USA) at the Institute for Environmental Genomics, University of Oklahoma, according to the manufacturer's instructions. The samples were prepared for sequencing using a TruSeq DNA kit according to the manufacturer's instructions. The purified mixture was diluted, denatured, rediluted, mixed with PhiX (equal to 30% of the final DNA amount), and then submitted to an Illumina MiSeq system for sequencing with the Reagent Kit v2 2 $\times$ 250 bp as described in the manufacturer's manual.

After sequencing, raw sequences were selected based on the sequence length, quality, primer, and tag using the Trimmomatic (version 0.35) and FLASH (version 1.2.11) programs (Bolger et al., 2014; Magoc & Salzberg, 2011). Sequencing reads of poor quality were removed by Btrim (Kong, 2011). Chimeras were removed by Uchime (Edgar et al., 2011). Reads that could not be

assembled were discarded. Sequences were then subjected to chimera detection using the Uchime algorithm (Edgar et al., 2011). Operational taxonomic units (OTUs) were classified at the 97% similarity level using Usearch (version 7.1), and the taxonomic assignment of OTUs was performed by the Ribosomal Database Project classifier with a minimal 70% confidence score (Wang et al., 2007). For the 16S rRNA gene, taxonomic assignment was performed using the Silva Release 119 database (Quast et al., 2013); for the ITS, the UNITE version 6.0 database was used (Koljalg et al., 2013).

## 2.4 | GeoChip 5.0 experiments and raw data analyses

GeoChip 5.0 was manufactured by Agilent (Agilent Technologies Inc., Santa Clara, CA, USA) in the 8 $\times$ 60 K format. A total of 600 ng of purified soil DNA from each sample was labelled with the fluorescent dye Cy-3 (GE Healthcare, CA, USA) using a random priming method as described previously (Tu et al., 2014), purified using a QIAquick Purification kit (Qiagen, CA, USA) and dried in a SpeedVac (Thermo Savant, NY, USA) into a powder. Subsequently, the labelled DNA was resuspended in 27.5  $\mu\text{L}$  of DNase/RNase-free distilled water and mixed completely with 42  $\mu\text{L}$  of hybridization solution containing 1 $\times$  Acgh blocking, 1 $\times$  HI-RPM hybridization buffer, 10 pM universal standard DNA, 0.05  $\mu\text{g}/\mu\text{L}$  Cot-1 DNA, and 10% formamide (final concentrations). Then, the solution was denatured at  $95^{\circ}\text{C}$  for 3 min, incubated at  $37^{\circ}\text{C}$  for 30 min, and hybridized with GeoChip 5.0 arrays (60 K). GeoChip hybridization was performed at  $67^{\circ}\text{C}$  in an Agilent hybridization oven for 24 h. After hybridization, the slides were washed using Agilent Wash Buffers at room temperature. Then, the arrays were scanned at 633 nm by a laser power of 100% and a photomultiplier tube gain of 75% with a NimbleGen MS200 Microarray Scanner (Roche NimbleGen, Inc., Madison, WI, USA). The image data were extracted by following the Agilent Feature Extraction program.

The microarray data were preprocessed by the microarray analysis pipeline on the IEG website (<http://ieg.ou.edu/microarray/>) as previously described (Tu et al., 2014). The main steps were as follows: (i) removing the spots of poor quality, which had a signal-to-noise ratio of less than 2.0; (ii) calculating the relative abundance of each soil sample by dividing the total intensity of the detected probes, then multiplying by a constant and taking the natural logarithm; and (iii) removing the detected probes in only two out of eight samples from the same sampling sites.

## 2.5 | Statistical analysis

Pearson correlation coefficients were calculated using SPSS 20.0 (SPSS, Inc., Chicago, IL, USA) and used to represent the relationship between carbon mineralization and the physicochemical properties or microbial biomass. Changes in environmental heterogeneity with

distance at four scales were estimated based on the soil physico-chemical properties and climatic factors (MAT and MAP) using the Bray–Curtis index. Richness and Shannon indexes based on OTUs for both bacterial and fungal communities were calculated and reflected by the  $\alpha$  diversity in the present study. The  $\beta$  diversity of both bacteria and fungi was ordinated based on the Bray–Curtis distance. The bacterial and fungal community structures at different sites were visualized using NMDS. The similarity matrices were built using the Bray–Curtis index. All of these analyses were conducted in R (<https://www.r-project.org/>) with the vegan package (Dixon, 2003).

The DDRs at the four spatial scales were estimated based on the  $\beta$  diversity of the microbial community with geographic distance (local scale (1–100m), mesoscale (0.5–50km), regional scale (100–3500km), and overall scale (1m–3500km)). The turnover rates ( $v$ ) were represented as the slope of the linear least squares regression of the relationship, which was calculated as follows:

$$v = \frac{\ln(1 - \beta \text{ diversity})}{\ln(\text{Geographic distance})} \quad (1)$$

To assess the statistical significance of turnover rates among the four spatial scales, a matrix permutation test was conducted with 999 permutations (McArdle & Anderson, 2001).

A random forest (RF) classification analysis was conducted to estimate the important predictors of both bacterial and fungal diversity among the variables soil pH, DOC,  $\text{NO}_3^-$ -N,  $\text{NH}_4^+$ -N, TN, TP, MAT, and MAP by determining how much the mean square error (MSE) increased when the data for a given predictor were permuted randomly while other predictors remained unchanged. Simultaneously, both bacterial and fungal  $\alpha$  diversity (Shannon index) and  $\beta$  diversity were used to estimate the effect of microbial diversity on carbon mineralization. The randomForest R package (Liaw & Wiener, 2002) was used to conduct these analyses, and the rfUtilities and rfPermute packages were used to assess the significance of the model and each predictor, respectively. Multiple comparisons (least significant difference, LSD) were used to calculate differences in the various indicators at different scales, such as microbial diversity (richness and Shannon index), soil physico-chemical properties, carbon mineralization, topological network parameters, and functional gene abundance. All data passed the normality test before the operation. The potential contribution of carbon functional genes to soil carbon mineralization at the four spatial scales was compared using RF analysis, and heatmaps were used to characterize the abundance of carbon degradation functional genes at the four scales. Heatmaps use colour changes to reflect data information in a two-dimensional matrix or table.

Based on the expected relationships among microbial community indexes and carbon mineralization, we developed the partial least squares path model (PLS-PM) (Dolce et al., 2018) linking  $\alpha$ -diversity,  $\beta$ -diversity, carbon functional gene, and carbon mineralization. The nonparametric bootstrapping (1000 resamples in this study) was used to estimate the precision of the PLS parameter estimates. The 95% bootstrap confidence interval was used to judge whether the estimated path coefficients were significant. The path coefficients

represent the direction and strength of the direct effects between the two variables. In addition, we calculated the standardized total effect of each potential variable. PLS-PM was performed using the package “pls” in R3.2.5 (Tenenhaus et al., 2005). The adjusted  $p$  values of multiple comparisons were calculated based on Benjamini–Hochberg multiple-testing correction by false discovery rate (FDR). The model's reliability was evaluated using the Goodness of Fit (GoF) statistic.

Co-occurrence networks were constructed to identify the specialists and generalists of bacterial or fungal taxa that dominantly contributed to carbon mineralization at different spatial scales by combining related functional genes and using RF analysis to determine the degree of linkage. The four spatial scales were defined as follows: local scale (1–100m) included 39 sampling network points (13 sites  $\times$  3 parallel points); mesoscale (0.5–50km) included 13 networks (13 sites); regional scale (100–3500km) was included 3 networks (three parallel), and overall scale (1m–3500km) was defined as 1 total network. Subsequently, the subnetworks at each local, meso, and regional scale were individually integrated, and the interrelationships among the co-occurrence networks across these four scales were depicted alongside the overall scale. Topology-based analysis of large networks was employed to understand the co-occurrence patterns in the microbial communities. Intrakingdom interaction networks for soil bacteria and fungi were constructed by using the Cytoscape software plugin (v 3.7.1, Co-occurrence network inference (CoNet) (Faust et al., 2012)). The OTUs of 429 samples were categorized into 4 groups based on the spatial scales as well as OTU annotation files, which were then uploaded and filtered by a minimum 1/3 threshold across the total OTUs. Subsequently, the Pearson, Spearman, Bray–Curtis, and Kullback–Leibler correlation methods were used to evaluate pairwise associations by CoNet (Faust et al., 2012; Machado et al., 2021). The initial thresholds for all four measures were selected to retrieve 1000 positive and 1000 negative edges. For each measure and edge, 1000 renormalized permutations and 1000 bootstrap scores were generated to alleviate compositionality bias. A measure-specific  $p$  value was computed first and then merged with Brown's method (Brown, 1975). Edges with merged  $p$  values less than .05 were retained after multiple testing using the Benjamini–Hochberg procedure (Benjamini & Hochberg, 1995). The co-occurrence networks were visualized with the interactive Gephi platform (0.9.2). The Euclidean distance of the network parameters was calculated to compare differences at the four spatial scales.

The weighted beta nearest taxon index ( $\beta$ NTI) and Bray–Curtis-based Raup–Crick (RCbray) values were calculated via a null model methodology to differentiate the ecological processes that regulate community assembly (Stegen et al., 2015). Specifically, deterministic processes include heterogeneous selection ( $\beta$ NTI  $> 2$ ) and homogeneous selection ( $\beta$ NTI  $< -2$ ); stochastic processes include homogeneous dispersal ( $|\beta$ NTI|  $< 2$ , RCbray  $< -0.95$ ), the dispersal limit ( $|\beta$ NTI|  $< 2$ , RCbray  $> 0.95$ ), and undominated processes ( $|\beta$ NTI|  $< 2$  and  $|\text{RCbray}| < 0.95$ ). These analyses were performed with the ‘picante’ and ‘vegan’ packages in R.



### 3 | RESULTS

#### 3.1 | Soil carbon mineralization and the distribution of the bacterial and fungal community structure and carbon degradation functional genes

Soil carbon mineralization was determined for all 429 samples across paddy fields in China (Figure 1a). These different patterns of carbon mineralization are closely related to complex environmental characteristics such as geographical patterns, climatic conditions, agricultural practices, soil types, and microbial activities. For example, at the northeastern sampling sites (HL, CC, and SY), the extent of soil carbon mineralization was  $16.31 \pm 2.71$ ,  $42.77 \pm 27.35$ , and  $23.92 \pm 17.53$  mg/(kg d), respectively; on the North China Plain (YY and FQ), the values increased to  $58.66 \pm 24.31$  and  $45.29 \pm 8.81$  mg/(kg d), respectively; in the Yangtze River's middle and lower reaches (HY, ZX, QZ, and LA), a fluctuating tendency was observed ( $40.57 \pm 23.82$ ,  $16.27 \pm 8.57$ ,  $57.76 \pm 17.49$ , and  $29.39 \pm 17.04$  mg/(kg d), respectively); and in the South China region (CT, JO, HK, and QX), the values progressively increased from  $38.07 \pm 20.61$  to  $40.57 \pm 23.82$ ,  $41.84 \pm 16.45$ , and  $52.14 \pm 24.18$  mg/(kg d). Taking soil attributes as an example, soil pH ranged from 3.56 to 8.65, and DOC ranged from 57.15 mg/kg to 509.83 mg/kg. The variation in the soil geochemical variables representing soil heterogeneity increased with spatial distance, i.e., local < meso < regional (Figure S1). Pearson's correlation was used to analyse the relationships between C mineralization and the soil properties and microbial biomass (Figure 1b, Table S2). C mineralization was significantly positively correlated with soil pH and DOC among all of the geochemical attributes measured ( $p < .05$ ) and highly correlated with bacterial biomass ( $p = .001$ ) and fungal biomass ( $p = .033$ ) at the latitudinal scale.

The total numbers of bacterial and fungal reads were 24,291,099 and 12,461,277, respectively, across all 429 samples. To minimize the impact of read count variation from different samples, all samples were resampled to 20,000 and 10,000 reads per sample for bacteria and fungi, respectively. A total of 70,145 operational taxonomic units (OTUs, 97% similarity cut-off) of the bacterial community and 49,165 OTUs (97% similarity) of the fungal community were identified. The soil microbial community diversity exhibited heterogeneity at the four spatial scales (Figure S2). For example, *Proteobacteria* was the dominant bacterial phylum ( $30.28 \pm 4.66\%$ ) at all sites, followed by *Cyanobacteria* ( $14.30 \pm 10.25\%$ ). *Mortierellomycota* was the dominant fungal phylum ( $54.67 \pm 26.30\%$ ) at all sites, followed by *Ascomycota* ( $19.58 \pm 11.20\%$ ). The soil microbial community showed significant regional distribution characteristics (Figure 2a, Table S3). The plots indicated that the composition of both soil bacteria and fungi showed significant regional differences associated with the climatic zone.

To better understand how microbial functional genes could impact the decomposition of SOC in different climatic zones, GeoChip 5.0 array high-throughput screening with integrated critically functional genes involved in various carbon cycling processes (Figure 2b) was performed. Carbon-degrading functional genes coding both

labile and resistant carbon degradation were profiled for all paddy samples. The results showed that the abundance of the functional genes involved in carbon degradation presented significant differences between bacteria (19 core genes) and fungi (19 core genes). For example, the functional genes in the bacterial groups were attributed more to proteins that encode starch-degrading genes, including *apu* ( $8.77 \pm 0.36$ , relative gene abundance), *cda* ( $568.04 \pm 1.17$ ), *nplT* ( $500.24 \pm 3.90$ ), and *pula* ( $764.29 \pm 1.45$ ), while those in the fungal groups were more associated with the degradation of recalcitrant carbon compounds, such as cellulose, hemicellulose, chitin, and lignin, including *exoglucanase* ( $554.59 \pm 1.11$ ), *xyla* ( $1.52 \pm 0.22$ ), *deacetylase* ( $737.79 \pm 1.19$ ), *ligninase* ( $1074.98 \pm 2.00$ ), and *mnp* ( $2210.32 \pm 3.61$ ). In addition, we used Pearson's correlation to analyse the relationship between bacterial and fungal diversity and their respective carbon functional genes (Figure S3). The  $\beta$  diversity of bacteria showed a significant positive correlation with carbon decomposition genes (14/19), while there were no significant differences between  $\alpha$  diversity and functional genes. For fungi, most of the carbon decomposition functional genes were positively correlated with  $\beta$  diversity (11/19), and only a few genes were negatively correlated with  $\alpha$  diversity (Shannon and richness index) (2/19). The findings suggest that both bacteria and fungi exhibit a significant positive correlation with the abundance of carbon functional genes (C-functional genes) at the spatial scale rather than within individual sampling sites. Furthermore, most of the functional genes related to carbon decomposition showed significant differences in the four climate zones, such as *amyA*, *glucoamylase*, *ara*, and *glx*, and the responses of bacteria and fungi were not completely consistent. The results indicated a series of specific traits and functions of the microbial community that might be responsible for the different routes to carbon metabolism.

#### 3.2 | Spatial turnovers of the soil microbial community structure and functional genes from local to regional scales

The distance decay relationship (DDR) of the soil microbial communities was examined at four spatial scales (local: 1–100 m, meso: 1–50 km, regional: 100–3500 km, and overall: 1 m–3500 km). A significant linear regression between the ln-transformed community similarities and geographic distance was observed for the bacterial and fungal communities ( $p < .01$ , Figure 3a,b). The spatial turnover rate of the fungal community was 2–4 times higher than that of the bacterial community at all spatial scales. Different microbial taxonomic spatial turnovers were further calculated at the phylum level (Figure S4, Table S4). The spatial scale dependence of DDR turnover in different phyla was consistent with that of the whole community. The spatial turnover rate was calculated using the slope of the DDR linear least square regression, revealing a hierarchical pattern of community heterogeneity, with bacterial and fungal communities exhibiting higher heterogeneity at larger spatial scales (regional > overall > meso > local).

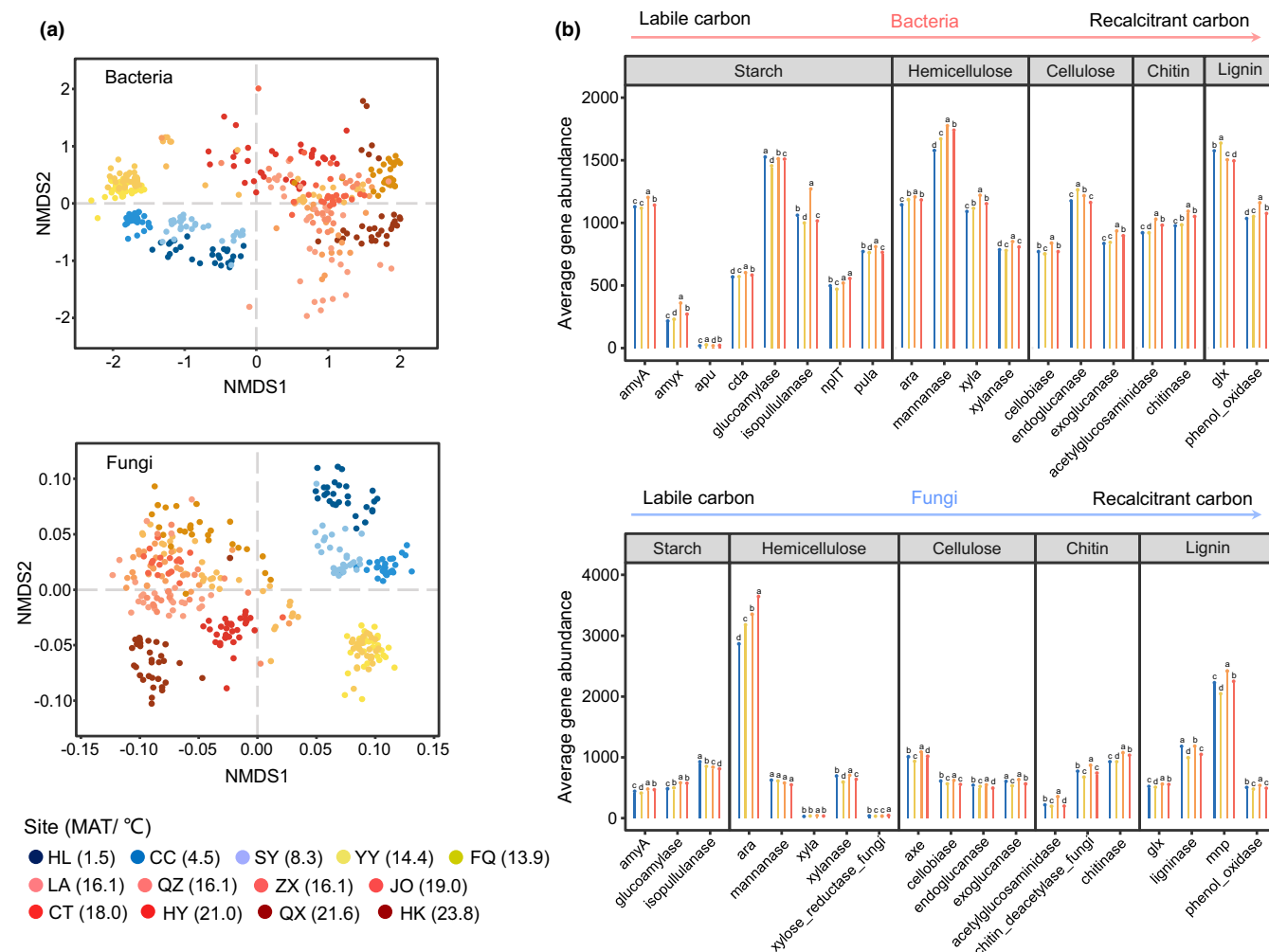


**FIGURE 2** Structure of bacterial and fungal communities and the abundances of functional genes involved in carbon mineralization. (a) Nonmetric multidimensional scaling (NMDS) of bacterial (above) and fungal (below) communities based on Bray–Curtis distances. Colours from dark blue (HL) to red (HK) represent samples across northern to southern China from 47.579°N to 19.758°N. (b) Columns represent the average abundance of functional genes involved in the decomposition of starch, hemicellulose, cellulose, chitin, and lignin in bacteria (above) and fungi (below) at middle temperate (blue), warm temperate (yellow), subtropical (orange), and tropical (red) temperatures. Error bars represent the standard deviation. Significant differences ( $p < .05$ ) in gene abundance in each climatic zone-paired group based on one-way ANOVA (multiple comparisons, Fisher's LSD test) are shown above the error bars.

Then, we analysed the microbial functional heterogeneity at the level of functional genes related to carbon decomposition (Figure 3c,d). Variations in microbial functional genes, such as *amyA*, *acetylglucosaminidase*, and *exoglucanase*, increased with geographical distance. In contrast to the community structure pattern, the highest functional heterogeneity occurred at the regional scale for bacteria and at the mesoscale for fungi. These results indicate that the functional genes involved in carbon decomposition change with increasing spatial distance. Random forest analysis was used to examine the contributions of environmental factors to bacterial and fungal  $\alpha$  and  $\beta$  diversities. The main drivers of microbial  $\alpha$  diversity varied at the four spatial scales (Figure S5a). Soil  $\text{NH}_4^+-\text{N}$  (13.4%) and TP (43.5%) were the main influential factors for bacteria at the local and meso scales, respectively. Soil  $\text{NO}_3^--\text{N}$  (24.8%) contributed most to fungal diversity at the meso scale, and no significant factors were found at the local scale. The influence of climatic factors

increased with spatial scale, with MAP and MAT contributing most to the variations in bacterial and fungal  $\alpha$  diversities at the regional and overall scales. In contrast, soil pH was the most important driver of bacterial  $\beta$  diversity at the four spatial scales (Figure S5b). The influence of MAP and MAT increased and contributed most to fungal  $\beta$  diversity at the regional and overall scales.

### 3.3 | Linkage of soil microbial structural and functional traits to soil carbon mineralization

Considering that the contribution of biodiversity and functional genes to carbon mineralization is influenced by both organismal characteristics and environmental factors, including climate variables (MAT and MAP), as well as environmental parameters (DOC and pH), we incorporated these factors into our model, along with

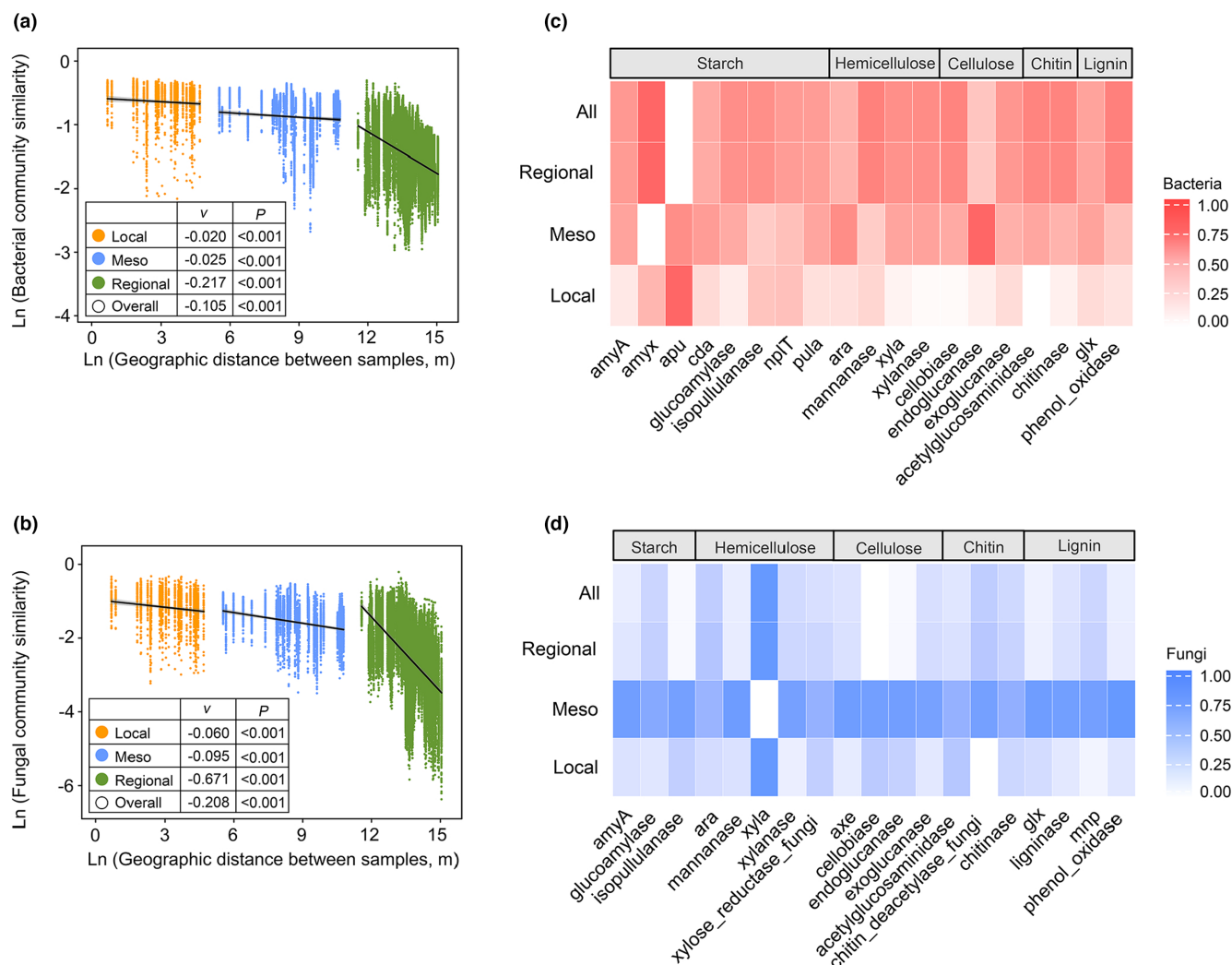


**FIGURE 3** Distance decay patterns indicating the community structural and carbon functional traits of soil bacteria and fungi at the four spatial scales. (a) Scatter plot representing the distance decay relationships (DDRs) of soil bacterial communities based on the Bray–Curtis distance at different spatial scales. The slope of the oblique line ( $v$ ) represents the microbial spatial turnover rate (Formula 1). Local: 1–100m; meso: 1–50km; regional: 100–3500km; and overall: 1m–3500km. (b) The DDRs of soil fungi at different spatial scales. (c) Heatmap of the variability of the carbon functional genes of bacteria at different spatial scales. (d) Variability of the carbon functional genes of fungi at different spatial scales.

$\alpha/\beta$  diversity and carbon decomposition gene data. Bacterial diversity (both  $\alpha$  and  $\beta$  diversity) had a greater impact on carbon mineralization at the four spatial scales than fungal diversity (Figure 4a,b). Bacterial and fungal  $\alpha$  and  $\beta$  diversity contributed most at the meso scale. The significant gene groups that contributed to carbon mineralization were *amyA*, *glucoamylase*, and *chitinase* for the bacterial community and *ara*, *cellobiase*, *chitin\_deacetylase*, *ligninase*, and *mnp* for the fungal community (Figure 4c,d). This result also indicates that bacterial functional genes mostly affected the labile carbon fraction, while fungal groups mainly affected the recalcitrant carbon fraction. We then constructed a structural equation model (SEM) using the partial least squares path analysis method (PLS-PM) with biodiversity (both  $\alpha$  and  $\beta$  diversity), functional genes, and heterotrophic respiration (equal to carbon mineralization) (Figure S6). Through analysis of the SEM, the bacterial carbon functional genes at different scales

had a correlation of 0.96 to 0.97 ( $p < .001$ ). The correlation between fungal carbon functional genes and carbon mineralization at the meso scale was  $-0.02$  ( $p < .001$ ). However, the effects of changes in spatial scale on species diversity were more pronounced. At the meso scale, the  $\beta$  diversity of bacteria and fungi contributed equal to 0.25 to carbon mineralization. As the scale increased, the contribution of  $\beta$  diversity decreased to less than 0.001. These findings suggest that the influence of spatial scaling on the microbial community is characterized by asynchronous variations in their functional traits, and the spatial scale effect has more influence on the composition of the microbial community than on its functional characteristics. Co-occurrence networks were constructed to link soil carbon mineralization and soil structural and functional traits together at different spatial scales (Figure 5, Table 1; Figure S7, Table S5). The dominance of bacterial taxa in the comprehensive functional network increased



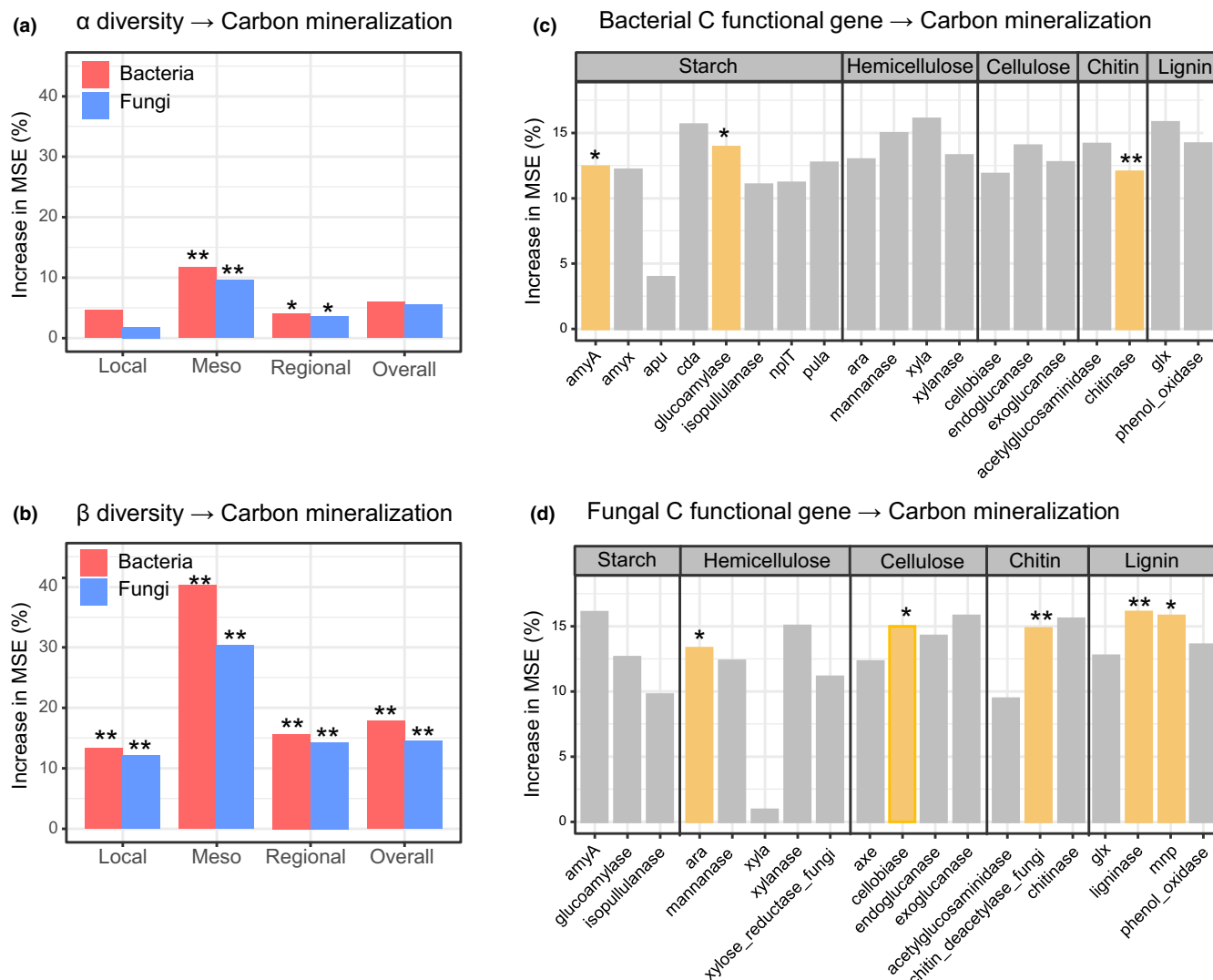


**FIGURE 4** Contribution of both biodiversity and functional gene diversity to carbon mineralization processes. Contribution of (a)  $\alpha$  diversity and (b)  $\beta$  diversity to carbon mineralization at four spatial scales. The average predictive values of bacterial and fungal diversity for carbon mineralization (% of increasing mean squared error (MSE)) were calculated by random forest (RF) analysis. Contributions of functional genes in (c) bacteria and (d) fungi to carbon mineralization are represented by the average predictive values. The significance levels of the predictors are as follows: \* $p < .05$ ; \*\* $p < .01$ .

proportionally with the spatial scale (from 63.20% to 83.67%). This observation aligns with the outcomes obtained from random forest analysis, indicating that bacteria make a greater contribution to carbon mineralization than fungi. Moreover, the network demonstrated the highest number of nodes (338) and edges (6277) at the meso scale, accompanied by a corresponding network heterogeneity value of 0.924. However, there was a significant decline in the total number of nodes entering the network as the spatial scale increased. The evident outcome is that no carbon decomposition functional genes were successfully integrated at both regional and overall scales. The top 10 OTUs were selected based on a weighted ranking in the local, meso, and regional scale subnetworks (Table S5). There was a significant increase in the abundance of generalist microorganisms as the spatial scale expanded. Notably, both bacteria and fungi within the top 10 taxa were generalist species at the regional scale. This finding

suggests that as the spatial scale increases, microbial interactions become more frequent and generalists can enhance their carbon decomposition capacity through functional complementarity. This finding also highlights the predominant influence of spatial scale on microbial community composition, surpassing its impact on functional genes associated with carbon decomposition.

## 4 | DISCUSSION

The strength of the relationship linking changes in biodiversity to changes in functional traits depends on scale (Bengtsson et al., 2002). In the present study, the spatial turnover rates of soil bacteria and fungi (at the phylum level) were approximately consistent with the spatial scaling effects in terms of the whole community

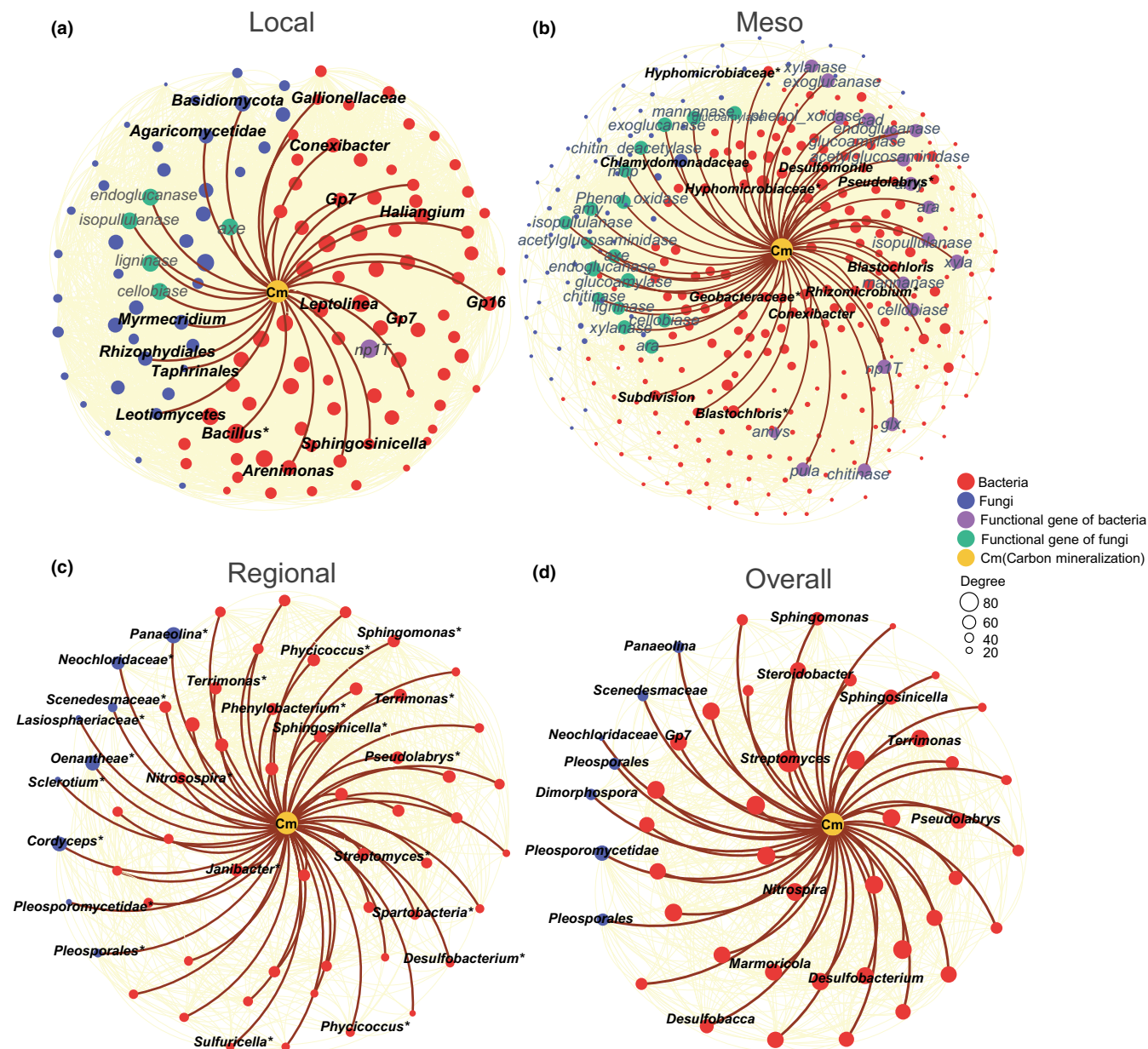


**FIGURE 5** Co-occurrence network analyses for carbon mineralization in the four spatial scales. The network pathway shows the fundamental linkages between functional bacterial and fungal communities and related genes associated with carbon mineralization. Each node (red or blue spot) in the four spatial scales represents an operational taxonomic unit (OTU, at the genus level) of bacteria or fungi that contributes to carbon mineralization (Cm), and each edge represents a positive or negative interaction. The size of each node represents the magnitude referred to as Cm, and the gradient colour of each edge represents the weight of significant regulation. The bold italic words indicate the top 10 OTUs (bacteria or fungi) contributing to Cm based on the weight scale. Genus\* represents the generalist taxon detected with a probability exceeding 50% among each subnetwork. The italicized words represent critical genes of bacteria (purple dots) and fungi (green dots) that regulate Cm processes.

(Figure 3a,b; Figure S3). However, functional gene variances related to carbon decomposition between bacteria and fungi were less dependent on spatial turnover, and the most significant contribution of carbon functional genes by bacteria and fungi occurred at the meso scale (Figure S6). The correlation between bacterial  $\alpha$  diversity and carbon functional genes exhibited a significant increase as the scale increased. The fungal diversity ( $\alpha$  and  $\beta$ ) remained the most prominent correlation at the meso scale. These findings indicate that

spatial scaling effects on the microbial community are asynchronous variations among their functional traits, and the spatial scale effect has more influence on the composition of the bacteria community than on its functional characteristics.

To explain the asynchronous variation between biodiversity and carbon mineralization functional traits, we propose two theories. The first is that probabilistic dispersal influences local dynamics. Thompson et al. (2017) showed that moderate dispersal can permit

TABLE 1 Properties of the bacterial and fungal co-occurrence networks in the paddy fields.

|          | Nodes |              |             | Edges |               |              | Network density | Clustering coefficient | Network centralization | Avg. number of neighbours | Network heterogeneity | Characteristic path length |
|----------|-------|--------------|-------------|-------|---------------|--------------|-----------------|------------------------|------------------------|---------------------------|-----------------------|----------------------------|
|          | Total | Bacteria     | Fungi       | Total | Positive      | Negative     |                 |                        |                        |                           |                       |                            |
| Local    | 125   | 79 (63.20%)  | 45 (36.00%) | 3848  | 3298 (85.71%) | 550 (14.29%) | 0.497           | 0.571                  | 0.249                  | 61.568                    | 0.232                 | 1.503                      |
| Meso     | 338   | 253 (74.85%) | 84 (24.85%) | 6277  | 6276 (99.98%) | 1 (0.02%)    | 0.110           | 0.343                  | 0.244                  | 37.142                    | 0.924                 | 2.463                      |
| Regional | 61    | 50 (81.97%)  | 10 (16.39%) | 788   | 513 (56.20%)  | 275 (43.80%) | 0.431           | 0.708                  | 0.589                  | 25.836                    | 0.406                 | 1.569                      |
| Overall  | 49    | 41 (83.67%)  | 7 (14.29%)  | 595   | 343 (57.65%)  | 252 (42.35%) | 0.506           | 0.746                  | 0.515                  | 24.286                    | 0.391                 | 1.494                      |

species to efficiently track spatial changes in the optimal environment and increase their functions. A previous study demonstrated that the probability of the dispersion of microorganisms decreased when the individuals were larger than 20 µm in diameter (Wilkinson et al., 2012), while microbes smaller than approximately 1 µm in diameter were not subject to dispersion (Finlay, 2002). The null model indicated that homogeneous dispersal (66.43% and 69.23%) and heterogeneous selection (32.40% and 30.77%) dominated the bacterial community composition at the local and meso scales. More undominated processes (57.69%) affected the bacterial community composition at the regional scale. This resulted in a decrease in homogeneous dispersal (17.95%) and heterogeneous selection (20.51%) (Figure S8). Bacteria are more susceptible to dispersal limitation than fungi due to their smaller size (size-hypothesis), resulting in the higher average functional abundance occurring in bacteria than in fungi at multiple scales. Movement from patch to patch by mobile consumers can stabilize the function (Loreau et al., 2003). The second hypothesis is that soil heterogeneity increases the range of environmental conditions (environmental filtering). Heterogeneity is a fundamental property of soil that underpins the emergence and maintenance of soil microbial diversity (Jansson & Hofmockel, 2020; Nunan et al., 2020). Moreover, heterogeneous soil also leads to the chemical heterogeneity of soil organic matter, which is the case for high-yield cropland at the landscape scale (Shi et al., 2018). Environmental filtering imposed by variable abiotic factors results in scenarios with high or low community turnover, depending on the consistency of these factors. In the present study, the influence of environmental factors (DOM and pH) on the  $\alpha$ -diversity of bacteria was greater than that of fungi at all spatial scales (Figure S5). DOM affects fundamental biogeochemical processes in the soil, such as nutrient cycling and organic matter storage (Roth et al., 2019). Soil microbiomes have a strong impact on DOM composition (Li et al., 2018), and bacteria have a greater effect on DOM composition than fungi (Roth et al., 2019). We hypothesized that some fungi, such as ectomycorrhizal fungi, preferentially degrade large rice-derived polymers (such as lignin) and partially mineralize and transform them into a diverse suite of small molecules that are subsequently consumed by bacteria during microbial processing. This process requires higher turnover for fungi than for bacteria, resulting in an increase in bacterial diversity (Liang et al., 2017).

Soil pH is another key factor influencing bacterial and fungal communities (Chu et al., 2010; Fierer & Jackson, 2006; Liu et al., 2014). In contrast to that of bacteria, the spatial distribution of soil fungi was associated with the soil pH, possibly because fungi are adapted to wider pH ranges than bacteria (Lauber et al., 2008; Rousk et al., 2010). Therefore, bacteria are more sensitive to environmental filtering (with low community turnover) than fungi at local spatial scales. In contrast, a recent study revealed that the spatial turnover of bacterial communities was greater than that of fungal communities in boreal forest soils (Ma et al., 2017). The relative importance of underlying factors (environmental variables or geographic distance) contributing to distance decay relationships (DDRs) also differs across different habitats, such as alpine grassland, desert,

desert grassland, typical grassland, and an entire transect (Wang et al., 2017). Natural ecosystems such as forests and bamboo forests are less disturbed by humans. Thus, soil fungal communities present more plant specificity than soil bacterial communities (Urbanova et al., 2015), especially rhizospheric fungi (Mummey & Rillig, 2006). Paddy fields are typical human-managed ecosystems, and bacterial dispersal limitation may be lower due to modern farming activities (Gao et al., 2019).

Consistent with their functional traits, bacteria contribute more than fungi during the process of carbon mineralization at multiple spatial scales. Irrespective of the community  $\alpha$  or  $\beta$  diversity, the random forest results showed that the involvement of bacteria in carbon metabolism was significantly greater than that of fungi (Figure 4a,b). The coexistence patterns between bacteria and fungi, induced by spatial scaling effects, serve as reliable indicators for bioassessment at the meso scale (Loreau, 2000).

Due to the potential dependence of microbial diversity on habitat type at different spatial scales (Lozupone & Knight, 2007; Zinger et al., 2014), microorganisms often exhibit characteristic specialization towards a localized resource patch or generalization towards a broader range of compounds (Allison et al., 2014). We further analysed the potential of bacteria and fungi to metabolize different carbon sources, ranging from labile to recalcitrant carbon. We found that the bacterial community contributed more to labile carbon decomposition (*amyA* and *glucoamylase*), while fungi were more involved in recalcitrant carbon degradation (*ara*, *cellobiase*, *chitin\_deacetylase*, *ligninase*, and *mnp*) (Figure 4c,d). Even for the metabolism of recalcitrant carbon, bacteria contributed 1.2 times as much as fungi to the related functional genes. This finding is consistent with previous studies showing that bacteria are the main decomposers of simple carbohydrates, organic acids, and amino acids, while fungi are more important for the decomposition of refractory soil carbon (Fontaine et al., 2011; Myers et al., 2001). The greater phylogenetic diversity and breadth of the metabolic capacities of bacteria appear to have a stronger effect on the decomposition of carbon compared with that of fungi (Glassman et al., 2018).

Bacteria and fungi have distinct substrate preferences and metabolic differences, and the co-occurrence of distinct roles of fungi or bacteria is central to understanding soil carbon mineralization (Rousk & Frey, 2015). In the present study, bacteria and fungi exhibited a variety of potential microbial interactions in paddy fields in China. The proportions of highly abundant bacteria and fungi related to carbon metabolism at the four spatial scales were as follows: local (bacteria = 63.20% vs. fungi = 36.00%), meso (bacteria = 74.85% vs. fungi = 24.85%), regional (bacteria = 81.97% vs. fungi = 16.39%), and overall (bacteria = 83.67% vs. fungi = 14.29%) (Figure 5 and Table 1). Bacteria were more strongly associated with carbon mineralization than fungi in the co-occurrence network, which is consistent with the strength of their functional traits at multiple scales being higher than that of fungi.

Bacteria and fungi share the same habitats and are therefore almost certain to frequently interact with each other in soil (Zhang et al., 2014). Therefore, based on coexistence theory, larger scales of

space encompass a greater range of environments, which increases species' opportunities for niche partitioning (Hart et al., 2017) and promotes spatial niche complementarity (Williams et al., 2017). We speculate that positive or negative co-occurrences may represent potential interactions in which individual interacting partners complement or compete during carbon processes at these spatial scales (de Menezes et al., 2017). The importance of competition as the major structural force could emerge; meanwhile, the community might be made up of several specialists, with each consuming a limited range of substrates, thus reducing the competition among each member of the community and increasing complementarity (Hooper et al., 2005). When the top 10 bacteria or fungi were sorted by weight, there was a discernible decline in specialist taxa as the spatial scale increased. Gravel et al. (2011) found that generalist assemblages were more productive across a range of carbon substrates because of their superior ability to exploit the imposed heterogeneity in the resource environment, while the slope of the biodiversity-ecosystem functioning (BEF) relationship was stronger for the assemblages of specialists because of the enhanced niche complementarity. The fact that the community of bacteria and fungi can underpin carbon metabolism via complementarity within and among soil niches means that spatial scale effects can generate a positive effect on carbon mineralization.

Soil organic carbon (SOC) is a nonrenewable resource that is currently being depleted at a faster rate than it is being formed (Lal, 2003). Any changes in either soil conditions or management practices will alter the geochemical or environmental chemical processes that subsequently impact the cycling of carbon and nitrogen in agroecosystems, which finally leads to the production of greenhouse gases (i.e.,  $\text{CH}_4$ ,  $\text{N}_2\text{O}$ , and  $\text{CO}_2$ ) (Li et al., 2004; Sass et al., 2002). With increases in crop-specific yields (240% increase in global dry biomass production) (Gray et al., 2014) facilitated by the development and adoption of improved cultivars and management accompanied by technological advances in the past 50 years, atmospheric  $\text{CO}_2$  has increased by as much as 50% in the Northern Hemisphere (Graven et al., 2013; Keeling et al., 1996). Increasing evidence has pointed to the role of soil microorganisms, which are important engines of decomposition and participate in terrestrial carbon source-sink dynamics (Glassman et al., 2018; Jansson & Hofmockel, 2020; Nunan et al., 2020; Tang et al., 2018). In the present study, pH and DOC were two abiotic factors that were positively correlated with carbon mineralization. Both of them participate in the processes of carbon conversion mediated by microorganisms via a series of redox reactions to exchange or provide unbound electrons (Chow et al., 2006; Cook & Allan, 1992; Lundquist et al., 1999), produce new oxidants (e.g.,  $\text{O}_2$ ,  $\text{NO}_3^-$ ,  $\text{Mn}^{4+}$ ,  $\text{Fe}^{3+}$  and  $\text{SO}_4^{2-}$ ) (Li et al., 2004), and consequently discharge greenhouse gases. However, in large-scale studies, we usually ignore the contribution of microorganisms to greenhouse gas emissions. This is because while these studies can test the underlying mechanisms at the local scale, they cannot also directly address theoretical predictions at a broader scale (Isbell et al., 2018; Thompson et al., 2018). Multiple scale measures can be used to predict the spatial patterns of turnover in microbial diversity



associated with functioning that are inherent to observational data, especially at large spatial scales (Gonzalez et al., 2020). Soil heterogeneity and spatial-scale effects have notable asynchronous effects on the microbial community composition and functional traits. They can also drive patterns of synchrony across large spatial scales based on niche complementarity. With larger datasets, including time series across a network of spatial locations in the future, we can increase our confidence in uncontrolled variables that co-vary with diversity and carbon mineralization functioning, and characterize the scales of synchrony and cross-coherence regarding species fluctuations at different levels.

Our study compared bacterial and fungal biogeographic patterns and carbon decomposition at four spatial scales, from the local scale to the continental scale. pH and DOC were two abiotic factors that were positively correlated with carbon mineralization. There is a trade-off in microbial traits that determines the proportion of microbial organic carbon invested in biosynthesis. Bacteria had a greater capacity for dispersal over different spatial scales than fungi based on the DDR, which represents a reasonable explanation for the relationship between microbial communities and soil organic matter metabolism. The bacterial community contributed more to carbon mineralization because the catabolic breadth of bacteria was more focused on labile carbon decomposition, while fungi were more involved in recalcitrant carbon degradation. Functional traits and microbial communities were influenced by spatial scaling effects and showed striking asynchrony. Niche complementarity can homogenize functional traits and promote the metabolism of carbon by microorganisms. With limited soil resources, the community is made up of several specialists, with each consuming a limited range of substrates. However, as the spatial scale increases, there is an escalating interaction among diverse generalist groups, leading to an accelerated carbon decomposition process. Overall, our study provides new insights for predicting the unique functional characteristics of the most diverse and complex microorganisms in spatial community ecology.

## AUTHOR CONTRIBUTIONS

All authors contributed intellectual input and assistance to this study and manuscript. Yuting Liang, Jizhong Zhou, and Bo Sun developed the original framework. Kaikai Zheng, Na Zhang, and Haowei Ni performed the sampling and experiments. Zhiyuan Ma, Kaikai Zheng, Haowei Ni, Dong Li, and Na Zhang analysed the data and prepared the figures. Zhiyuan Ma and Shuo Jiao wrote the paper with comments from Yunfeng Yang, Jizhong Zhou, and Yuting Liang.

## ACKNOWLEDGEMENTS

We would like to thank Xishu Zhou, Qingyun Yan, Sai Zhou, Feng Wang, and Xiangtian Meng for sampling and experimental assistance. This study was supported by National Natural Science Foundation of China (42107146, 42377121), Natural Science Foundation of Jiangsu Province (BK20210994), Innovation Program of Institute of Soil Science (ISSASIP2201), and the Youth Innovation Promotion Association of Chinese Academy of Sciences.

## CONFLICT OF INTEREST

All authors declare that they have no competing interests.

## DATA AVAILABILITY STATEMENT

Raw sequence data for 16S rRNA and ITS gene amplicons were deposited under NCBI BioProject Accession No. PRJNA562601 and No. PRJNA562792, respectively. The GeoChip data are available in the repository Figshare, <https://doi.org/10.6084/m9.figshare.9746303>.

## ORCID

Zhiyuan Ma  <https://orcid.org/0000-0001-5694-2214>

Shuo Jiao  <https://orcid.org/0000-0002-1228-1757>

Na Zhang  <https://orcid.org/0000-0001-7848-025X>

Yunfeng Yang  <https://orcid.org/0000-0001-8274-6196>

Yuting Liang  <https://orcid.org/0000-0001-5443-4486>

## REFERENCES

- Adair, E. C., Parton, W. J., Del Grosso, S. J., Silver, W. L., Harmon, M. E., Hall, S. A., Burke, I. C., & Hart, S. C. (2008). Simple three-pool model accurately describes patterns of long-term litter decomposition in diverse climates. *Global Change Biology*, 14(11), 2636–2660. <https://doi.org/10.1111/j.1365-2486.2008.01674.x>
- Allison, S. D., Chacon, S. S., & German, D. P. (2014). Substrate concentration constraints on microbial decomposition. *Soil Biology & Biochemistry*, 79, 43–49. <https://doi.org/10.1016/j.soilbio.2014.08.021>
- Bengtsson, J., Engelhardt, K., Giller, P., Hobbie, S., Lawrence, D., Levine, J., Vila, M., & Wolters, V. (2002). Slippin' and slidin' between the scales: The scaling components of biodiversity-ecosystem functioning relations. In M. Loreau, S. Naeem, & P. Inchausti (Eds.), *Biodiversity and ecosystem functioning: Synthesis and perspectives* (pp. 209–220). Oxford University Press.
- Benjamini, Y., & Hochberg, Y. (1995). Controlling the false discovery rate – A practical and powerful approach to multiple testing. *Journal of the Royal Statistical Society Series B-Statistical Methodology*, 57(1), 289–300. <https://doi.org/10.1111/j.2517-6161.1995.tb02031.x>
- Bolger, A. M., Lohse, M., & Usadel, B. (2014). Trimmomatic: A flexible trimmer for Illumina sequence data. *Bioinformatics*, 30(15), 2114–2120. <https://doi.org/10.1093/bioinformatics/btu170>
- Bossio, D. A., & Scow, K. M. (1998). Impacts of carbon and flooding on soil microbial communities: Phospholipid fatty acid profiles and substrate utilization patterns. *Microbial Ecology*, 35(3), 265–278. <https://doi.org/10.1007/s002489900082>
- Bremner, J. M. (1965). Total nitrogen, inorganic forms of nitrogen, organic forms of nitrogen. In C. A. Black (Ed.), *Method of soil analysis* (Vol. 2, pp. 1149–1178). American Society of Agronomy.
- Brown, M. B. (1975). 400: A method for combining non-independent, one-sided tests of significance. *Biometrics*, 31(4), 987–992. <https://doi.org/10.2307/2529826>
- Bruehlheide, H., Dengler, J., Purschke, O., Lenoir, J., Jimenez-Alfaro, B., Hennekens, S. M., Botta-Dukát, Z., Chytrý, M., Field, R., Jansen, F., Kattge, J., Pillar, V. D., Schrod, F., Mahecha, M. D., Peet, R. K., Sandel, B., van Bodegom, P., Altman, J., Alvarez-Dávila, E., ... Jandt, U. (2018). Global trait-environment relationships of plant communities. *Nature Ecology & Evolution*, 2(12), 1906–1917. <https://doi.org/10.1038/s41559-018-0699-8>
- Chow, A. T., Tanji, K. K., Gao, S. D., & Dahlgren, R. A. (2006). Temperature, water content and wet-dry cycle effects on DOC production and carbon mineralization in agricultural peat soils. *Soil Biology & Biochemistry*, 38(3), 477–488. <https://doi.org/10.1016/j.soilbio.2005.06.005>



- Chu, H. Y., Fierer, N., Lauber, C. L., Caporaso, J. G., Knight, R., & Grogan, P. (2010). Soil bacterial diversity in the Arctic is not fundamentally different from that found in other biomes. *Environmental Microbiology*, 12(11), 2998–3006.
- Cook, B. D., & Allan, D. L. (1992). Dissolved organic-carbon in old field soils - compositional changes during the biodegradation of soil organic-matter. *Soil Biology & Biochemistry*, 24(6), 595–600. [https://doi.org/10.1016/0038-0717\(92\)90085-C](https://doi.org/10.1016/0038-0717(92)90085-C)
- de Menezes, A. B., Richardson, A. E., & Thrall, P. H. (2017). Linking fungal-bacterial co-occurrences to soil ecosystem function. *Current Opinion in Microbiology*, 37, 135–141. <https://doi.org/10.1016/j.mib.2017.06.006>
- Degnan, P. H., & Ochman, H. (2012). Illumina-based analysis of microbial community diversity. *The ISME Journal*, 6(1), 183–194. <https://doi.org/10.1038/ismej.2011.74>
- Dixon, P. (2003). VEGAN, a package of R functions for community ecology. *Journal of Vegetation Science*, 14(6), 927–930. <https://doi.org/10.1111/j.1654-1103.2003.tb02228.x>
- Dolce, P., Vinzi, V. E., & Lauro, N. C. (2018). Non-symmetrical composite-based path modeling. *Advances in Data Analysis and Classification*, 12(3), 759–784. <https://doi.org/10.1007/s11634-017-0302-1>
- Edgar, R. C., Haas, B. J., Clemente, J. C., Quince, C., & Knight, R. (2011). UCHIME improves sensitivity and speed of chimera detection. *Bioinformatics*, 27(16), 2194–2200. <https://doi.org/10.1093/bioinformatics/btr381>
- Falkowski, P. G., Fenchel, T., & Delong, E. F. (2008). The microbial engines that drive Earth's biogeochemical cycles. *Science*, 320(5879), 1034–1039. <https://doi.org/10.1126/science.1153213>
- Faust, K., Sathirapongsasuti, J. F., Izard, J., Segata, N., Gevers, D., Raes, J., & Huttenhower, C. (2012). Microbial co-occurrence relationships in the human microbiome. *PLoS Computational Biology*, 8(7), e1002606. <https://doi.org/10.1371/journal.pcbi.1002606>
- Fierer, N., & Jackson, R. B. (2006). The diversity and biogeography of soil bacterial communities. *Proceedings of the National Academy of Sciences of the United States of America*, 103(3), 626–631. <https://doi.org/10.1073/pnas.0507535103>
- Finlay, B. J. (2002). Global dispersal of free-living microbial eukaryote species. *Science*, 296(5570), 1061–1063. <https://doi.org/10.1126/science.1070710>
- Fontaine, S., Henault, C., Aamor, A., Bdioui, N., Bloor, J. M. G., Maire, V., Mary, B., Revalliot, S., & Maron, P. A. (2011). Fungi mediate long term sequestration of carbon and nitrogen in soil through their priming effect. *Soil Biology & Biochemistry*, 43(1), 86–96. <https://doi.org/10.1016/j.soilbio.2010.09.017>
- Gao, Q., Yang, Y. F., Feng, J. J., Tian, R. M., Guo, X., Ning, D. L., Hale, L., Wang, M., Cheng, J., Wu, L., Zhao, M., Zhao, J., Wu, L., Qin, Y., Qi, Q., Liang, Y., Sun, B., Chu, H., & Zhou, J. Z. (2019). The spatial scale dependence of diazotrophic and bacterial community assembly in paddy soil. *Global Ecology and Biogeography*, 28(8), 1093–1105. <https://doi.org/10.1111/geb.12917>
- Glassman, S. I., Weihe, C., Li, J., Albright, M. B. N., Looby, C. I., Martiny, A. C., Treseder, K. K., Allison, S. D., & Martiny, J. B. H. (2018). Decomposition responses to climate depend on microbial community composition. *Proceedings of the National Academy of Sciences of the United States of America*, 115(47), 11994–11999. <https://doi.org/10.1073/pnas.1811269115>
- Gonzalez, A., Germain, R. M., Srivastava, D. S., Filotas, E., Dee, L. E., Gravel, D., Thompson, P. L., Isbell, F., Wang, S., Kéfi, S., Montoya, J., Zelnik, Y. R., & Loreau, M. (2020). Scaling-up biodiversity-ecosystem functioning research. *Ecology Letters*, 23(4), 757–776. <https://doi.org/10.1111/ele.13456>
- Gravel, D., Bell, T., Barbera, C., Bouvier, T., Pommier, T., Venail, P., & Mouquet, N. (2011). Experimental niche evolution alters the strength of the diversity-productivity relationship. *Nature*, 469(7328), 89–92. <https://doi.org/10.1038/nature09592>
- Graven, H. D., Keeling, R. F., Piper, S. C., Patra, P. K., Stephens, B. B., Wofsy, S. C., Welp, L. R., Sweeney, C., Tans, P. P., Kelley, J. J., Daube, B. C., Kort, E. A., Santoni, G. W., & Bent, J. D. (2013). Enhanced seasonal exchange of CO<sub>2</sub> by northern ecosystems since 1960. *Science*, 341(6150), 1085–1089. <https://doi.org/10.1126/science.1239207>
- Gray, J. M., Frolking, S., Kort, E. A., Ray, D. K., Kucharik, C. J., Ramankutty, N., & Friedl, M. A. (2014). Direct human influence on atmospheric CO<sub>2</sub> seasonality from increased cropland productivity. *Nature*, 515(7527), 398–401. <https://doi.org/10.1038/nature13957>
- Green, J. L., Holmes, A. J., Westoby, M., Oliver, I., Briscoe, D., Dangerfield, M., Gillings, M., & Beattie, A. J. (2004). Spatial scaling of microbial eukaryote diversity. *Nature*, 432(7018), 747–750. <https://doi.org/10.1038/nature03034>
- Griffiths, R. I., Thomson, B. C., James, P., Bell, T., Bailey, M., & Whiteley, A. S. (2011). The bacterial biogeography of British soils. *Environmental Microbiology*, 13(6), 1642–1654. <https://doi.org/10.1111/j.1462-2920.2011.02480.x>
- GRISIP, G.R.S.P., (2013). Rice Almanac, fourth ed. International Rice Research Institute, Los Ban'os (Philippines), p. 283.
- Grundmann, G. L., & Debouzie, D. (2000). Geostatistical analysis of the distribution of NH<sub>4</sub><sup>+</sup> and NO<sub>2</sub><sup>-</sup>-oxidizing bacteria and serotypes at the millimeter scale along a soil transect. *FEMS Microbiology Ecology*, 34(1), 57–62. <https://doi.org/10.1111/j.1574-6941.2000.tb00754.x>
- Haney, R. L., Brinton, W. H., & Evans, E. (2008). Estimating soil carbon, nitrogen, and phosphorus mineralization from short-term carbon dioxide respiration. *Communications in Soil Science and Plant Analysis*, 39(17–18), 2706–2720. <https://doi.org/10.1080/00103620802358862>
- Hart, S. P., Usinowicz, J., & Levine, J. M. (2017). The spatial scales of species coexistence. *Nature Ecology & Evolution*, 1(8), 1066–1073.
- Hooper, D. U., Chapin, F. S., Ewel, J. J., Hector, A., Inchausti, P., Lavorel, S., Lawton, J. H., Lodge, D. M., Loreau, M., Naeem, S., Schmid, B., Setälä, H., Symstad, A. J., Vandermeer, J., & Wardle, D. A. (2005). Effects of biodiversity on ecosystem functioning: A consensus of current knowledge. *Ecological Monographs*, 75(1), 3–35. <https://doi.org/10.1890/04-0922>
- Horner-Devine, M. C., Lage, M., Hughes, J. B., & Bohannan, B. J. (2004). A taxa-area relationship for bacteria. *Nature*, 432(7018), 750–753. <https://doi.org/10.1038/nature03073>
- Isbell, F., Cowles, J., Dee, L. E., Loreau, M., Reich, P. B., Gonzalez, A., Hector, A., & Schmid, B. (2018). Quantifying effects of biodiversity on ecosystem functioning across times and places. *Ecology Letters*, 21(6), 763–778. <https://doi.org/10.1111/ele.12928>
- Jackson, L. E., Calderon, F. J., Steenwerth, K. L., Scow, K. M., & Rolston, D. E. (2003). Responses of soil microbial processes and community structure to tillage events and implications for soil quality. *Geoderma*, 114(3–4), 305–317. [https://doi.org/10.1016/S0016-7061\(03\)00046-6](https://doi.org/10.1016/S0016-7061(03)00046-6)
- Jansson, J. K., & Hofmockel, K. S. (2020). Soil microbiomes and climate change. *Nature Reviews. Microbiology*, 18(1), 35–46. <https://doi.org/10.1038/s41579-019-0265-7>
- Jiao, S., Xu, Y. Q., Zhang, J., & Lu, Y. H. (2019). Environmental filtering drives distinct continental atlases of soil archaea between dryland and wetland agricultural ecosystems. *Microbiome*, 7, 15. <https://doi.org/10.1186/s40168-019-0630-9>
- Keeling, C. D., Chin, J. F. S., & Whorf, T. P. (1996). Increased activity of northern vegetation inferred from atmospheric CO<sub>2</sub> measurements. *Nature*, 382(6587), 146–149. <https://doi.org/10.1038/382146a0>
- Koljalg, U., Nilsson, R. H., Abarenkov, K., Tedersoo, L., Taylor, A. F., Bahram, M., Bates, S. T., Bruns, T. D., Bengtsson-Palme, J., Callaghan, T. M., Douglas, B., Drenkhan, T., Eberhardt, U., Dueñas, M., Grebenc, T., Griffith, G. W., Hartmann, M., Kirk, P. M., Kohout, P., ... Larsson, K.

- H. (2013). Towards a unified paradigm for sequence-based identification of fungi. *Molecular Ecology*, 22(21), 5271–5277. <https://doi.org/10.1111/mec.12481>
- Kong, Y. (2011). Btrim: A fast, lightweight adapter and quality trimming program for next-generation sequencing technologies. *Genomics*, 98(2), 152–153. <https://doi.org/10.1016/j.ygeno.2011.05.009>
- Lal, R. (2003). Soil erosion and the global carbon budget. *Environment International*, 29(4), 437–450. [https://doi.org/10.1016/S0160-4120\(02\)00192-7](https://doi.org/10.1016/S0160-4120(02)00192-7)
- Lal, R. (2004). Soil carbon sequestration impacts on global climate change and food security. *Science*, 304(5677), 1623–1627. <https://doi.org/10.1126/science.1097396>
- Lauber, C. L., Strickland, M. S., Bradford, M. A., & Fierer, N. (2008). The influence of soil properties on the structure of bacterial and fungal communities across land-use types. *Soil Biology & Biochemistry*, 40(9), 2407–2415. <https://doi.org/10.1016/j.soilbio.2008.05.021>
- Lee, C. K., Barbier, B. A., Bottos, E. M., McDonald, I. R., & Cary, S. C. (2012). The inter-valley soil comparative survey: The ecology of dry valley edaphic microbial communities. *The ISME Journal*, 6(5), 1046–1057. <https://doi.org/10.1038/ismej.2011.170>
- Li, C. S., Mosier, A., Wassmann, R., Cai, Z. C., Zheng, X. H., Huang, Y., Tsuruta, H., Boonjawat, J., & Lantin, R. (2004). Modeling greenhouse gas emissions from rice-based production systems: Sensitivity and upscaling. *Global Biogeochemical Cycles*, 18(1), GB1043. <https://doi.org/10.1029/2003gb002045>
- Li, H. Y., Wang, H., Wang, H. T., Xin, P. Y., Xu, X. H., Ma, Y., Liu, W.-P., Teng, C.-Y., Jiang, C.-L., Lou, L.-P., Arnold, W., Cralle, L., Zhu, Y.-G., Chu, J.-F., Gilbert, J. A., & Zhang, Z. J. (2018). The chemodiversity of paddy soil dissolved organic matter correlates with microbial community at continental scales. *Microbiome*, 6(1), 187. <https://doi.org/10.1186/s40168-018-0561-x>
- Liang, C., Schimel, J. P., & Jastrow, J. D. (2017). The importance of anabolism in microbial control over soil carbon storage. *Nature Microbiology*, 2(8), 17105. <https://doi.org/10.1038/nmicrobiol.2017.105>
- Liaw, A., & Wiener, M. (2002). Classification and regression by random Forest. *R News*, 2(3), 18–22.
- Liu, J. J., Sui, Y. Y., Yu, Z. H., Shi, Y., Chu, H. Y., Jin, J., Liu, X., & Wang, G. H. (2014). High throughput sequencing analysis of biogeographical distribution of bacterial communities in the black soils of northeast China. *Soil Biology & Biochemistry*, 70, 113–122. <https://doi.org/10.1016/j.soilbio.2013.12.014>
- Liu, J. J., Sui, Y. Y., Yu, Z. H., Shi, Y., Chu, H. Y., Jin, J., Liu, X., & Wang, G. H. (2015). Soil carbon content drives the biogeographical distribution of fungal communities in the black soil zone of northeast China. *Soil Biology & Biochemistry*, 83, 29–39. <https://doi.org/10.1016/j.soilbio.2015.01.009>
- Loreau, M. (2000). Are communities saturated? On the relationship between  $\alpha$ ,  $\beta$  and  $\gamma$  diversity. *Ecology Letters*, 3(2), 73–76.
- Loreau, M., Mouquet, N., & Gonzalez, A. (2003). Biodiversity as spatial insurance in heterogeneous landscapes. *Proceedings of the National Academy of Sciences of the United States of America*, 100(22), 12765–12770. <https://doi.org/10.1073/pnas.2235465100>
- Lozupone, C. A., & Knight, R. (2007). Global patterns in bacterial diversity. *Proceedings of the National Academy of Sciences of the United States of America*, 104(27), 11436–11440. <https://doi.org/10.1073/pnas.0611525104>
- Lundquist, E. J., Jackson, L. E., & Scow, K. M. (1999). Wet-dry cycles affect dissolved organic carbon in two California agricultural soils. *Soil Biology & Biochemistry*, 31(7), 1031–1038. [https://doi.org/10.1016/S0038-0717\(99\)00017-6](https://doi.org/10.1016/S0038-0717(99)00017-6)
- Ma, B., Dai, Z. M., Wang, H. Z., Dsouza, M., Liu, X. M., He, Y., Wu, J., Rodrigues, J. L., Gilbert, J. A., Brookes, P. C., & Xu, J. M. (2017). Distinct biogeographic patterns for archaea, bacteria, and fungi along the vegetation gradient at the continental scale in eastern China. *mSystems*, 2(1), e00174–16. <https://doi.org/10.1128/mSystems.00174-16>
- Magoc, T., & Salzberg, S. L. (2011). FLASH: Fast length adjustment of short reads to improve genome assemblies. *Bioinformatics*, 27(21), 2957–2963. <https://doi.org/10.1093/bioinformatics/btr507>
- Matchado, M. S., Lauber, M., Reitmeier, S., Kacprowski, T., Baumbach, J., Haller, D., & List, M. (2021). Network analysis methods for studying microbial communities: A mini review. *Computational and Structural Biotechnology Journal*, 19, 2687–2698. <https://doi.org/10.1016/j.csbj.2021.05.001>
- Mazurkiewicz, P., Tang, C. M., Boone, C., & Holden, D. W. (2006). Signature-tagged mutagenesis: Barcoding mutants for genome-wide screens. *Nature Reviews. Genetics*, 7(12), 929–939. <https://doi.org/10.1038/nrg1984>
- McArdle, B. H., & Anderson, M. J. (2001). Fitting multivariate models to community data: A comment on distance-based redundancy analysis. *Ecology*, 82(1), 290–297. [https://doi.org/10.1890/0012-9658\(2001\)082\[0290:Fmmtcd\]2.0.Co;2](https://doi.org/10.1890/0012-9658(2001)082[0290:Fmmtcd]2.0.Co;2)
- Mummey, D. L., & Rillig, M. C. (2006). The invasive plant species *Centaurea maculosa* alters arbuscular mycorrhizal fungal communities in the field. *Plant and Soil*, 288(1–2), 81–90. <https://doi.org/10.1007/s11104-006-9091-6>
- Myers, R. T., Zak, D. R., White, D. C., & Peacock, A. (2001). Landscape-level patterns of microbial community composition and substrate use in upland forest ecosystems. *Soil Science Society of America Journal*, 65(2), 359–367. <https://doi.org/10.2136/sssaj2001.652359x>
- Ning, D., Yuan, M., Wu, L., Zhang, Y., Guo, X., Zhou, X., Yang, Y., Arkin, A. P., Firestone, M. K., & Zhou, J. (2020). A quantitative framework reveals ecological drivers of grassland microbial community assembly in response to warming. *Nature Communications*, 11(1), 4717. <https://doi.org/10.1038/s41467-020-18560-z>
- Nunan, N., Schmidt, H., & Raynaud, X. (2020). The ecology of heterogeneity: Soil bacterial communities and C dynamics. *Philosophical Transactions of the Royal Society of London. Series B, Biological Sciences*, 375(1798), 20190249. <https://doi.org/10.1098/rstb.2019.0249>
- Nunan, N., Wu, K., Young, I. M., Crawford, J. W., & Ritz, K. (2002). In situ spatial patterns of soil bacterial populations, mapped at multiple scales, in an arable soil. *Microbial Ecology*, 44(4), 296–305. <https://doi.org/10.1007/s00248-002-2021-0>
- Quast, C., Pruesse, E., Yilmaz, P., Gerken, J., Schweer, T., Yarza, P., Peplies, J., & Glockner, F. O. (2013). The SILVA ribosomal RNA gene database project: Improved data processing and web-based tools. *Nucleic Acids Research*, 41(Database issue), D590–D596. <https://doi.org/10.1093/nar/gks1219>
- Ritz, K., McNicol, J. W., Nunan, N., Grayston, S., Millard, P., Atkinson, D., Kollotte, A., Habeshaw, D., Boag, B., Clegg, C. D., Griffiths, B. S., Wheatley, R. E., Glover, L. A., McCaig, A. E., & Prosser, J. I. (2004). Spatial structure in soil chemical and microbiological properties in an upland grassland. *FEMS Microbiology Ecology*, 49(2), 191–205. <https://doi.org/10.1016/j.femsec.2004.03.005>
- Roth, V. N., Lange, M., Simon, C., Hertkorn, N., Bucher, S., Goodall, T., Griffiths, R. I., Mellado-Vázquez, P. G., Mommer, L., Oram, N. J., Weigelt, A., Dittmar, T., & Gleixner, G. (2019). Persistence of dissolved organic matter explained by molecular changes during its passage through soil. *Nature Geoscience*, 12(9), 755–761. <https://doi.org/10.1038/s41561-019-0417-4>
- Rousk, J., Baath, E., Brookes, P. C., Lauber, C. L., Lozupone, C., Caporaso, J. G., Knight, R., & Fierer, N. (2010). Soil bacterial and fungal communities across a pH gradient in an arable soil. *The ISME Journal*, 4(10), 1340–1351. <https://doi.org/10.1038/ismej.2010.58>
- Rousk, J., & Frey, S. D. (2015). Revisiting the hypothesis that fungal-to-bacterial dominance characterizes turnover of soil organic matter and nutrients. *Ecological Monographs*, 85(3), 457–472. <https://doi.org/10.1890/14-1796.1>

- Sass, R. L., Andrews, J. A., Ding, A. J., & Fisher, F. M. (2002). Spatial and temporal variability in methane emissions from rice paddies: Implications for assessing regional methane budgets. *Nutrient Cycling in Agroecosystems*, 64(1–2), 3–7. <https://doi.org/10.1023/A:1021107016714>
- Shi, Y., Li, Y., Xiang, X., Sun, R., Yang, T., He, D., Zhang, K., Ni, Y., Zhu, Y.-G., Adams, J. M., & Chu, H. (2018). Spatial scale affects the relative role of stochasticity versus determinism in soil bacterial communities in wheat fields across the North China Plain. *Microbiome*, 6(1), 27. <https://doi.org/10.1186/s40168-018-0409-4>
- Stegen, J. C., Lin, X., Fredrickson, J. K., & Konopka, A. E. (2015). Estimating and mapping ecological processes influencing microbial community assembly. *Frontiers in Microbiology*, 6, 370. <https://doi.org/10.3389/fmicb.2015.00370>
- Tang, Z., Sun, X., Luo, Z., He, N., & Sun, O. J. (2018). Effects of temperature, soil substrate, and microbial community on carbon mineralization across three climatically contrasting forest sites. *Ecology and Evolution*, 8(2), 879–891. <https://doi.org/10.1002/ece3.3708>
- Tedersoo, L., Bahram, M., Toots, M., Diedhiou, A. G., Henkel, T. W., Kjöller, R., Morris, M. H., Nara, K., Nouhra, E., Peay, K. G., Pölme, S., Ryberg, M., Smith, M. E., & Koljalg, U. (2012). Towards global patterns in the diversity and community structure of ectomycorrhizal fungi. *Molecular Ecology*, 21(17), 4160–4170. <https://doi.org/10.1111/j.1365-294X.2012.05602.x>
- Tenenhaus, M., Vinzi, V. E., Chatelin, Y. M., & Lauro, C. (2005). PLS path modeling. *Computational Statistics & Data Analysis*, 48(1), 159–205. <https://doi.org/10.1016/j.csda.2004.03.005>
- Thompson, P. L., Isbell, F., Loreau, M., O'Connor, M. I., & Gonzalez, A. (2018). The strength of the biodiversity-ecosystem function relationship depends on spatial scale. *Proceedings of the Biological Sciences*, 285, 20180038. <https://doi.org/10.1098/rspb.2018.0038>
- Thompson, P. L., Rayfield, B., & Gonzalez, A. (2017). Loss of habitat and connectivity erodes species diversity, ecosystem functioning, and stability in metacommunity networks. *Ecography*, 40(1), 98–108. <https://doi.org/10.1111/ecog.02558>
- Tu, Q., Yu, H., He, Z., Deng, Y., Wu, L., Van Nostrand, J. D., Zhou, A., Voordeckers, J., Lee, Y. J., Qin, Y., Hemme, C. L., Shi, Z., Xue, K., Yuan, T., Wang, A., & Zhou, J. (2014). GeoChip 4: A functional gene-array-based high-throughput environmental technology for microbial community analysis. *Molecular Ecology Resources*, 14(5), 914–928. <https://doi.org/10.1111/1755-0998.12239>
- Urbanova, M., Snajdr, J., & Baldrian, P. (2015). Composition of fungal and bacterial communities in forest litter and soil is largely determined by dominant trees. *Soil Biology & Biochemistry*, 84, 53–64. <https://doi.org/10.1016/j.soilbio.2015.02.011>
- Wang, Q., Garrity, G. M., Tiedje, J. M., & Cole, J. R. (2007). Naive Bayesian classifier for rapid assignment of rRNA sequences into the new bacterial taxonomy. *Applied and Environmental Microbiology*, 73(16), 5261–5267. <https://doi.org/10.1128/AEM.00062-07>
- Wang, X. B., Lu, X. T., Yao, J., Wang, Z. W., Deng, Y., Cheng, W. X., Zhou, J. Z., & Han, X. G. (2017). Habitat-specific patterns and drivers of bacterial beta-diversity in China's drylands. *The ISME Journal*, 11(6), 1345–1358. <https://doi.org/10.1038/ismej.2017.11>
- Wilkinson, D. M., Koumoutsaris, S., Mitchell, E. A. D., & Bey, I. (2012). Modelling the effect of size on the aerial dispersal of microorganisms. *Journal of Biogeography*, 39(1), 89–97. <https://doi.org/10.1111/j.1365-2699.2011.02569.x>
- Williams, L. J., Paquette, A., Cavender-Bares, J., Messier, C., & Reich, P. B. (2017). Spatial complementarity in tree crowns explains overyielding in species mixtures. *Nature Ecology & Evolution*, 1(4), 63. <https://doi.org/10.1038/s41559-016-0063>
- Xiao, D., Huang, Y., Feng, S. Z., Ge, Y. H., Zhang, W., He, X. Y., & Wang, K. L. (2018). Soil organic carbon mineralization with fresh organic substrate and inorganic carbon additions in a red soil is controlled by fungal diversity along a pH gradient. *Geoderma*, 321, 79–89. <https://doi.org/10.1016/j.geoderma.2018.02.003>
- Yao, H., Campbell, C. D., Chapman, S. J., Freitag, T. E., Nicol, G. W., & Singh, B. K. (2013). Multi-factorial drivers of ammonia oxidizer communities: Evidence from a national soil survey. *Environmental Microbiology*, 15(9), 2545–2556. <https://doi.org/10.1111/1462-2920.12141>
- Yim, M. H., Joo, S. J., & Nakane, K. (2002). Comparison of field methods for measuring soil respiration: A static alkali absorption method and two dynamic closed chamber methods. *Forest Ecology and Management*, 170(1–3), 189–197. [https://doi.org/10.1016/S0378-1127\(01\)00773-3](https://doi.org/10.1016/S0378-1127(01)00773-3)
- Zhang, M., Pereira e Silva Mde, C., Chaib De Mares, M., & van Elsas, J. D. (2014). The mycosphere constitutes an arena for horizontal gene transfer with strong evolutionary implications for bacterial-fungal interactions. *FEMS Microbiology Ecology*, 89(3), 516–526. <https://doi.org/10.1111/1574-6941.12350>
- Zhou, J., Bruns, M. A., & Tiedje, J. M. (1996). DNA recovery from soils of diverse composition. *Applied and Environmental Microbiology*, 62(2), 316–322. <https://doi.org/10.1128/aem.62.2.316-322.1996>
- Zhou, J., He, Z., Yang, Y., Deng, Y., Tringe, S. G., & Alvarez-Cohen, L. (2015). High-throughput metagenomic technologies for complex microbial community analysis: Open and closed formats. *MBio*, 6(1), e02288-14. <https://doi.org/10.1128/mBio.02288-14>
- Zinger, L., Boetius, A., & Ramette, A. (2014). Bacterial taxa-area and distance-decay relationships in marine environments. *Molecular Ecology*, 23(4), 954–964. <https://doi.org/10.1111/mec.12640>

## SUPPORTING INFORMATION

Additional supporting information can be found online in the Supporting Information section at the end of this article.

**How to cite this article:** Ma, Z., Jiao, S., Zheng, K., Ni, H., Li, D., Zhang, N., Yang, Y., Zhou, J., Sun, B., & Liang, Y. (2023). Multiple spatial scales of bacterial and fungal structural and functional traits affect carbon mineralization. *Molecular Ecology*, 00, 1–16. <https://doi.org/10.1111/mec.17235>